Myosin VIIA is a marker for the cone accessory outer segment in zebrafish

Hodel, Corinne ; Niklaus, Stephanie ; Heidemann, Martina ; Klooster, Jan ; Kamermans, Maarten ; Biehlmaier, Oliver ; Gesemann, Matthias ; Neuhauss, Stephan C F

DOI: https://doi.org/10.1002/ar.22976

Myosin VIIA is a Marker for the Cone Accessory Outer Segment in Zebrafish

Corinne Hodel[1], Stephanie Niklaus[1], Martina Heidemann[1,2], Jan Klooster[3], Maarten Kamermans[3], Oliver Biehlmaier[1,4], Matthias Gesemann[1,*], Stephan CF Neuhauss[1,*]

[1]Institute of Molecular Life Sciences, University of Zurich, Winterthurerstrasse 190, CH–8057 Zurich, Switzerland
[2]Current address: Department of Physiology, University of Bern, Bühlplatz 5, CH–3012 Bern, Switzerland
[3]Netherlands Institute for Neuroscience, The Royal Netherlands Academy of Arts and Sciences, Meibergdreef 47, NL–1105 BA Amsterdam, The Netherlands
[4]Current address: Biozentrum, University of Basel, Klingelbergstrasse 50/70, CH-4056 Basel, Switzerland

* Corresponding authors: matthias.gesemann@imsl.uzh.ch or stephan.neuhauss@imls.uzh.ch

Contact: Prof. Stephan Neuhauss; Institute of Molecular Life Sciences, University of Zurich, Winterthurerstrasse 190, CH–8057 Zurich, Switzerland; +41 44 635 6040 (phone); +41 44 635 6817 (fax)

Running title: Accessory Outer Segment of Zebrafish Cones

Grant sponsor: Swiss National Science Foundation; Grant number: 31003A-117782.

Keywords: Accessory outer segment, Myosin VIIa, cone photoreceptor, zebrafish

Abstract

The accessory outer segment, a cytoplasmic structure running alongside the photoreceptor outer segment has been described in teleost fishes, excluding the model organism zebrafish. So far the function of the accessory outer segment is unknown.

Here we describe the ultrastructure of the zebrafish cone accessory outer segment by electron microscopy. Starting at the connecting cilium the accessory outer segment runs parallel alongside the cone outer segment. A thin plasma bridge connects the outer segment with the accessory outer segment, whose surface is enlarged by foldings and invaginations. Beside the morphological descriptions, we demonstrate that the Usher protein Myosin VIIa (Myo7a) is a specific marker for the zebrafish cone accessory outer segment.

Zebrafish cone photoreceptors possess a large and well differentiated accessory outer segment, in which the unconventional motor protein Myo7a is highly enriched. The direct cytoplasmic contact with the cone outer segment as well as the surface enlargement of the accessory outer segment suggests an important role of this structure in transport and exchange of metabolites between the cone outer segment and the surrounding retinal pigment epithelium. In future studies of the outer retina more attention should be paid to this often neglected structure.

Abbreviations

AOS, accessory outer segment; CC, connecting cilium; COS, cone outer segment; CP, calycal process; Myo7a, Myosin VIIA; RPE, retinal pigment epithelium; SEM, scanning electron microscopy; TEM, transmission electron microscopy

Introduction

The zebrafish (*Danio rerio*) is an important model organism to investigate the vertebrate visual system (Gestri et al., 2012). Being diurnal vertebrates, zebrafish are advantageous to study cone vision. Here, we describe a highly visible but little studied structure of the zebrafish cone photoreceptor, the accessory outer segment (AOS).

The AOS was first described by Engström (Engström, 1961) in the family of Gadidae (cods) as a cilium-like structure with a fine netlike cytoplasm, but even 50 years after its initial description, the function of the AOS is still unknown. Historically, this structure is referred to as 'accessory element' (Engström, 1963) or 'lateral sac' (Fineran and Nicol, 1974), but is now more commonly referred to as accessory outer segment. The structure has been described in several teleost species. It originates from the connecting cilium which is located between the photoreceptor inner and outer segment and runs along the outer segment. AOS and cone outer segment are connected via a thin plasma bridge enclosed by a continuous membrane (Engström, 1963; Fineran and Nicol, 1974; Nagle et al., 1986; Yacob et al., 1977). In teleost double cones both have their own AOS (Engström, 1961; Januschka et al., 1987).

In this study, we show that retinal expression of Myo7a in adult zebrafish is restricted to the AOS. Myo7a is an unconventional myosin (Cheney and Mooseker, 1992). In mammals, MYO7A is expressed in cochlear and vestibular sensory hair cells of the inner ear and in photoreceptor cilia and retinal pigment epithelium (RPE) (el-Amraoui et al., 1996; Hasson et al., 1995; Liu et al., 1997; Weil et al., 1996; Wolfrum et al., 1998). Moreover, in species having calycal processes such as primates or frogs, Myo7a is also expressed in this supporting photoreceptor structure (Sahly et al., 2012). In zebrafish wild-type larvae *myo7a* has been found in the inner ear and in neuromast

hair cells, but not in the eye (Ernest et al., 2000). *MYO7A* mutations in humans lead to Usher syndrome 1B characterized by sensorineural vision and hearing loss (Usher, 1914). The *Myo7a* mouse mutant *shaker-1* (Gibson et al., 1995) shows an eye phenotype including opsin accumulation in the connecting cilium (Liu et al., 1999), abnormal phagocytoses in the RPE (Gibbs et al., 2003), and impaired pigment granule movements (Liu et al., 1998). In zebrafish, *myo7a* has been identified as the defective gene in the *mariner* mutant (Ernest et al., 2000). *mariner* mutants belong to the circler mutants, characterized by balance impairments (Nicolson et al., 1998; Sahly et al., 2012).

Here, in addition to the selective AOS marker Myo7a, we also present for the first time a detailed ultrastructural analysis of the zebrafish cone AOS.

Material and Methods

Fish maintenance

Both adult and larval wild-type zebrafish (*Danio rerio*) were kept under a 14 hour/10 hour light/dark cycle at 28°C. Larvae were staged according to days post fertilisation and raised in E3 medium. Adult fish were older than three months.

Electron microscopy

For scanning electron microscopy (SEM) the samples were conserved in freshly prepared fixative (1% paraformaldehyde, 100mM phosphate buffer, 3% saccharose, 0.15mM $CaCl_2$-solution and 2.5% glutaraldehyde) over night at 4°C and washed with 100mM sodium cacodylate buffer. Postfixation with 2% osmium tetroxide for 30 minutes at room temperature was followed by washing with 100mM sodium cacodylate buffer and a graded ethanol series ending with a H_2O-free absolute ethanol step. Samples were transferred to critical point drying device (Bal-Tec AG, today Leica Microsystems). After several medium changes between dry ethanol and fluid CO_2 at around 10°C, samples were dried above the critical point of CO_2. Before the dried specimens were mounted on carbon pads, they were broken by means of a razor blade or a tungsten wire. In order to avoid charging the samples when exposed to electrons, the surface was covered with a 10-20nm thick platinum or gold coat by means of a sputter coater (Bal-Tec AG, today Leica Microsystems). Samples were analysed with the Zeiss SUPRA 50 VP scanning electron microscope.

For standard transmission electron microscopy (TEM) the same fixation was used as for scanning electron microscopy. Samples were subsequently washed with 100mM phosphate buffer before postfixation in 1% osmium tetroxide for 80 minutes at room temperature. Then samples were washed with 100mM

phosphate buffer, followed by ddH_2O before contrasting with 1% uranyl acetate for 1 hour at 4°C. Dehydration was done in a graded ethanol series and a propylene oxide step. After preinfiltration in an epon/propylene oxide mixture, samples were embedded in pure epon and polymerized at 65°C for 24-48 hours. Ultrathin sections were contrasted with Reynolds lead citrate for 15 minutes and analysed with a Philips CM208 transmission electron microscope.

TEM immunohistochemistry has been done as described in detail by Klooster et al. (2009). Briefly, after fixation and cryoprotection, 40µm thick frozen sections were incubated with the polyclonal rabbit α-Myo7a antibody for 48 hours. After rinsing, the sections were incubated in a PowerVisionPoly-HRP-Goat α-rabbit IgG (ImmunoVision Technologies Co.) To visualize the peroxidase, the sections were incubated in a Tris-HCl diaminobenzidine (DAB) solution containing 0.03% H_2O_2. The DAB reaction product was then intensified by a gold-substituted silver peroxidase method (Jordan et al., 1996). Sections were postfixed in 1% OsO_4 supplemented with 1% potassium ferricyanide in sodium cacodylate buffer 0.1M (pH 7.4). Sections were dehydrated and embedded in epoxy resin. Ultrathin sections were observed and photographed in a FEI Tecnai 12 electron microscope.

Fluorescence immunohistochemistry

Adult wild-type zebrafish were sacrificed, the eye cup was removed and immediately fixed (without lens) in 2% trichloracetic acid for 45 minutes at room temperature. After washing with 150mM phosphate-buffered saline (PBS, pH 7.4), the eye cup was cryoprotected in 30% sucrose at 4°C over night, embedded in Tissue-Tek (Sakura Finetek Germany GmbH) and frozen in liquid nitrogen. Sections with a thickness of 16µm were cut, mounted on SuperFrost®Plus slides (Menzel-Gläser) and air dried at 37°C before freezing at -20°C. Before the staining

procedure slides were thawed at 37°C and washed with PBS. In order to avoid background staining the slides were treated with a blocking solution (20% normal goat serum, 2% bovine serum albumin in PBS containing 0.3% Triton X-100) for at least 30 minutes at room temperature. The primary antibody diluted in blocking solution was applied over night at 4°C. The zebrafish Myo7a protein was stained with a rabbit α-Myo7a antibody (1:350, custom made by Eurogentec S.A., Seraing, Belgium) directed against a C-terminal peptide at position 2004-2017 (YRVKFEDDKSHFPS). Peptide designing was based on the protein sequence published by Ernest and colleagues (2000). Antibody specificity was tested in the presence of 3ng/µl Myo7a peptide to block staining to the Myo7a epitope. Washing with PBS was followed by incubation with a secondary antibody (AlexaFluor® 488, Invitrogen) diluted in PBS. The slides were washed and coverslipped with Mowiol and viewed with a Leica HCS LSI confocal microscope. Actin staining was performed on adult eyes, fixed with 2% paraformaldehyde for 30 minutes at room temperature. Cryoprotection, embedding and sectioning were carried out as described for immunohistochemistry. Sections were washed twice for 5 minutes with PBS and permeabilized for 45 minutes with PBS containing 0.3% Triton X-100. Phalloidin-FITC (Sigma-Aldrich) (1:200 in PBS containing 0.3% Triton X-100) was applied for 1 hour at room temperature. After washing, sections were coverslipped with Mowiol and imaged with a Leica HCS LSI confocal microscope.

Cloning and expression of Myo7a Ferm2 fragment

Zebrafish cDNA was essentially done as previously described in (Gesemann et al., 2010). The FERM2 domain of zebrafish Myo7a1 was amplified using the following primers: Myo7a1_dr_Kozak5572s GCCACC**ATG**GAGGTGGAGGCCATTC and Myo7a1_dr_6540as

TCACTTGCTGCTGCCG. 40 Cyles of amplifications were done using the Fast cycling polymerase (Qiagen). The amplified fragment was gel-purified and ligated into the pcDNA 3.3-Topo eukaryotic expression vector and several colonies were sequenced. Clones with no mutations and correct orientation were chosen for recombinant protein expression. 293T cells were transfected using the calcium-phosphate transfection method (Jordan et al., 1996). Cells were washed with PBS and subsequently lysed using SDS-Page sample buffer (50mM Tris pH 6.8; 2% SDS; 10% Glycerol, 12.5mM EDTA; 200mg/l bromphenolblue) 48h after transfection. DNA aggregates were broken by sonication and the lysate was cleared by centrifugation (5 minutes, 20000g). The recovered supernatant was used for western blot analysis.

Western blot analysis

Zebrafish lysates for western blot analysis were prepared from zebrafish eye and fin tissue using the following parameters: Four adult zebrafish eyes or an equivalent volume of zebrafish fin tissue were transferred to 1ml of SDS-PAGE sample buffer and homogenized using an Eppendorf tube pistil. Cells and DNA was further fragmented using sonication. Lysates were cleared using centrifugation and the supernatant was subjected to western blot analysis. Tissue and 293 lysates were separated on 4-15% Mini PROTEAN-TGX gels (Bio-Rad) and blotted to Invitrolon PVDF membranes (Invitrogen). Membranes were saturated by incubation with 3% dry milk powder in PBS+0.05% Tween20 (PBS-mT) for 2 hours. Subsequently the membranes were incubated with the Myo7a peptide antibody (1:1000) for 45 minutes at room temperature. Following 3 washes with PBS-mT membranes were incubated with a secondary donkey α-rabbit HRP conjugated antibody (1:100000; Jackson Immuno Research) for 90 minutes at room temperature. Following 4 washes with PBS-mT and one wash with PBS, membranes were

briefly rinsed with dH_2O and subjected to ECL solution (Thermo Scientific). Blots were exposed for 10 minutes in an ImageQuant LAS-4000 imaging system (GE Healthcare Lifescience) and the obtained images were analysed and adjusted using the Photoshop software.

Results and Discussion

Adult zebrafish cones feature an accessory outer segment

The AOS has been described in several teleost fish species. However, no studies in the model organism *Danio rerio* are yet available. In order to identify and resolve the AOS in zebrafish we used scanning electron microscopy (SEM) (Fig. 1A-C). The overview SEM picture (Fig. 1A) illustrates that every cone in the adult zebrafish retina is indeed associated with an AOS, which originates at the connecting cilium (CC). The CC in zebrafish is short and only visible as a small fissure. This is a marked difference to mammalian photoreceptors where inner and outer segments are spatially separated from each other and exclusively linked by the CC. The AOS is clearly smaller in diameter than the outer segment but larger than the calycal processes (CP) which longitudinally wrap every cone. The numerous and thin CP were about equidistantly distributed all around the cone from the outer limiting membrane to the outer segment. This basket-like structure formed by many CP was proposed to structurally stabilize the outer segment (Lin-Jones and Burnside, 2007; Pagh-Roehl et al., 1992). Higher optical magnification revealed the fine texture of the AOS (Fig. 1B, C). Its membrane appeared strongly ruffled with multiple foldings and invaginations, resulting in a huge surface enlargement.

We performed TEM to gain additional ultrastructural data. TEM sections (Fig. 1D–E) confirmed the findings obtained by SEM. The AOS continues from the CC leading to a gradual transition between CC and AOS. As suggested by the SEM

images, the AOS appeared to be continuous with the cytoplasm of the CC, running alongside the outer segment (Fig. 1D). Within the adult zebrafish cone outer segment (COS) there was no cytoplasmic part as the discs span all along the entire width of a radially sectioned outer segment. This is in contrast to mammalian COS which have a cytoplasmic part but are devoid of an AOS. This hints at the origin of the mammalian arrangement, in which the thin cytoplasmic bridge connecting the AOS and COS has been enlarged over time finally incorporating the AOS into the COS. In contrast to the CC (Fig. 1E), the AOS is devoid of microtubules (Fig. 2C). Nevertheless, the AOS membrane was irregularly curved leading to an enlarged surface confirming the SEM images. The membrane enclosing the AOS is part of the cell membrane as there is a cytoplasmic connection between the AOS and the COS. When analysing larval zebrafish, a rudimentary AOS could already be detected. However, no surface enlargement could be seen in 5 day (Fig 2A) or 12 day old larva (Fig. 2B), suggesting that differentiation at these stages is incomplete and that maturation occurs only at later stages. In larval as well as adult zebrafish, CP are separated from the COS, since they are enclosed by distinct membranes. Moreover, both AOS and RPE membranes run in parallel resulting in a close contact of these two structures. It has been proposed that an exchange of metabolites (for instance retinoids) takes place between RPE and cones via the AOS (Burnside et al., 1993; Yacob et al., 1977).

When analysing the electromicrographs, the enlarged surface of the AOS is consistent with such an assumption. The close contact of AOS and RPE has been suggested to stabilise the outer retina, especially during retinomotor movement activity (Fineran and Nicol, 1974; Yacob et al., 1977; Januschka et al., 1987; Burnside et al., 1993; Collin et al., 1996). Within a cone the AOS is thought to exchange metabolites, conduct signals from the inner to the outer segment, or the AOS could be a storage

compartment for metabolites (Januschka et al., 1987; Yacob et al., 1977; Fineran and Nicol, 1974).

Myo7a is a marker for the accessory outer segment

Until now there was no specific marker known to label the AOS. Since the unconventional motor protein Myo7a (for structure see Fig. 4A) is often associated with ciliary structures (Wolfrum et al., 1998), we raised peptide antibodies against zebrafish Myo7a to test the association of this protein with the AOS.

On adult retinal sections, fluorescence microscopy reveals a distinct Myo7a staining in the photoreceptor layer (Fig. 3). This labelling originated at the boundary of the inner and outer segment of every cone photoreceptor type alongside the outer segment, indicating that the AOS is indeed labelled. The staining of the AOS can be abolished by competition with the Myo7a peptide (Fig. 4B) indicating that the antibody indeed recognizes Myo7a. Moreover, the antibody did interact with a 260kD band in zebrafish retina extracts and recognizes the recombinant FERM2 domain of zebrafish Myo7a (Fig. 4C) further confirming its specificity. Consistent with our histological studies which have demonstrated that the AOS is not mature at 12 days post fertilization, we did not detect Myo7a staining in larval zebrafish eyes, suggesting that Myo7a serves as a selective marker for the mature AOS.

We also determined protein expression at the ultrastructural level using the same Myo7a-specific antibody previously employed for the fluorescence microscopical approach for transmission electron microscopical immunohistochemistry. These immunogold transmission electron microscopical studies confirmed the staining pattern found by means of fluorescence immunohistochemistry. The majority of gold particles were detected in the AOS (Fig. 5A). No particles could be seen in the cone outer or inner segment. A low number of gold particles were

found in the CC where the staining of the AOS faded out (Fig. 5B). These findings support the conclusion that our custom made antibody against the zebrafish Myo7a is a specific marker for the AOS in the adult zebrafish retina.

The role of Myo7a in the AOS is not known. However, participation in opsin transport is likely. Interestingly, a putative transport within the AOS seems to be rather independent of filamentous actin, as staining with labelled phalloidin, a marker for F-actin, did not highlight the AOS (Fig. 4D). In mice, it has been proposed that MYO7A is indeed involved in the transport of opsin from the inner to the outer segment. In the *Myo7a* mouse mutant known as *shaker-1* this transport is slower than in wild-type mice, leading to the accumulation of opsin in the inner segment (Liu et al., 1997). This finding ist consistent with MYO7A being involved in the transport of opsin through the cilium (Liu et al., 1999; Williams, 2002), but this accumulation may also be a secondary effect of phagocytosis defects of RPE cells (Hashimoto et al., 2007).

Myo7a has been found in the RPE of several species such as mouse, human, guinea pig, chicken or macaque (Liu et al., 1997; el-Amraoui et al., 1996). Interestingly, other than the AOS, we saw no staining with our antibody either in the zebrafish RPE or in any other part of the photoreceptor. However, a comprehensive study dealing with the expression of several Myosin proteins in fish retinae (including zebrafish, albino trout (*Oncorhynchus mykiss*), green sunfish (*Lepomis cynellus*) and striped bass (*Morone saxatilis*)) found Myo7a staining in the AOS but the antibody labelled also other parts of the photoreceptor and in other retinal cell types (Lin-Jones et al., 2009). As teleost genomes experienced a third whole genome duplication subsequent to the two vertebrate duplications (Amores et al., 1998; Postlethwait et al., 1998) the discrepancy may be explained by the fact that the zebrafish genome harbours two Myo7a paralogs. While our antibody was specifically raised

against the zebrafish Myo7a1 protein, the antibody used by Lin-Jones (Lin-Jones et al., 2009) is directed against the human myo7a ortholog, recognizing most likely both zebrafish Myo7a paralogs, Myo7a1 as well as Myo7a2. One is identical to the published sequence, located on chromosome 18 (Ernest et al., 2000), whereas another copy can be found on chromosome 21. The discovery of a second paralog may lead to a scenario where one paralog functions in photoreceptors, while the other may exert its function in the RPE.

In the mouse there is clear evidence that Myo7a indeed plays different roles. In photoreceptors the protein is involved in the transport of opsin (Liu et al., 1997), while in the RPE it is involved in the movement of organelles, such as phagosomes (Gibbs et al., 2003) and pigment granules (Schwander et al., 2009; Liu et al., 1998). Accordingly, in zebrafish Myo7a1 may fulfil its task in photoreceptors whereas Myo7a2 may act in the RPE. Alternatively, since in mice MYO7A exists as a monomer in photoreceptors, and as a dimer in RPE (Williams and Lopes, 2011), dimerization may prevent the access of our antibody to the epitope in the RPE.

In conclusion, the zebrafish accessory outer segment is a very prominent structure of the cone photoreceptor. So far it has received little attention, but it might prove to be an important structure for transport and exchange of metabolites between the cone inner and outer segment as well as with the surrounding retinal pigment epithelium. The unconventional myosin Myo7a1 is highly enriched in the accessory outer segment and can be used as a specific marker for studying this structure in greater details.

Acknowledgements

We thank Franziska Baumann and Kara Dannenhauer for excellent technical help and Dr. Beat Kunz for his support in recombinant protein expression.

Literature Cited

Amores A, Force A, Yan YL, Joly L, Amemiya C, Fritz A, Ho RK, Langeland J, Prince V, Wang YL, Westerfield M, Ekker M, Postlethwait JH. 1998. Zebrafish hox clusters and vertebrate genome evolution. Science 282:1711–1714.

Burnside B, Wang E, Pagh-Roehl K, Rey H. 1993. Retinomotor movements in isolated teleost retinal cone inner-outer segment preparations (CIS-COS): effects of light, dark and dopamine. Exp Eye Res 57:709–722.

Cheney RE, Mooseker MS. 1992. Unconventional myosins. Curr Opin Cell Biol 4:27–35.

Collin SP, Collin HB, Ali MA. 1996. Ultrastructure and organisation of the retina and pigment epithelium in the cutlips minnow, Exoglossum maxillingua (Cyprinidae, Teleostei). Histol Histopathol 11:55–69.

el-Amraoui A, Sahly I, Picaud S, Sahel J, Abitbol M, Petit C. 1996. Human Usher 1B/mouse shaker-1: the retinal phenotype discrepancy explained by the presence/absence of myosin VIIA in the photoreceptor cells. Hum Mol Genet 5:1171–1178.

Engström K. 1961. Cone types and cone arrangement in the retina of some gadids. Acta Zoologica 42:227–243.

Engström K. 1963. Cone types and cone arrangements in teleost retinae. Acta Zoologica 44:179–243.

Ernest S, Rauch GJ, Haffter P, Geisler R, Petit C, Nicolson T. 2000. Mariner is defective in myosin VIIA: a zebrafish model for human hereditary deafness. Hum Mol Genet 9:2189–2196.

Fineran BA, Nicol JA. 1974. Studies on the eyes of New Zealand parrot-fishes (Labridae). Proc R Soc Lond B Biol Sci 186:217–247.

Gesemann M, Lesslauer A, Maurer CM, Schönthaler HB, Neuhauss, Stephan C F. 2010. Phylogenetic analysis of the vertebrate excitatory/neutral amino acid transporter (SLC1/EAAT) family reveals lineage specific subfamilies. BMC Evol. Biol. 10:117.

Gestri G, Link BA, Neuhauss, Stephan C F. 2012. The visual system of zebrafish and its use to model human ocular diseases. Dev Neurobiol 72:302–327.

Gibbs D, Kitamoto J, Williams DS. 2003. Abnormal phagocytosis by retinal pigmented epithelium that lacks myosin VIIa, the Usher syndrome 1B protein. Proc Natl Acad Sci U S A 100:6481–6486.

Gibson F, Walsh J, Mburu P, Varela A, Brown KA, Antonio M, Beisel KW, Steel KP, Brown SD. 1995. A type VII myosin encoded by the mouse deafness gene shaker-1. Nature 374:62–64.

Hasson T, Heintzelman MB, Santos-Sacchi J, Corey DP, Mooseker MS. 1995. Expression in cochlea and retina of myosin VIIa, the gene product defective in Usher syndrome type 1B. Proc Natl Acad Sci U S A 92:9815–9819.

Hashimoto T, Gibbs D, Lillo C, Azarian SM, Legacki E, Zhang XM, Yang XJ, Williams DS. 2007. Lentiviral gene replacement

therapy of retinas in a mouse model for Usher syndrome type 1B. Gene Ther 14:584-94

Januschka MM, Burkhardt DA, Erlandsen SL, Purple RL. 1987. The ultrastructure of cones in the walleye retina. Vision Res 27:327–341.

Jordan M, Schallhorn A, Wurm FM. 1996. Transfecting mammalian cells: optimization of critical parameters affecting calcium-phosphate precipitate formation. Nucleic Acids Res. 24:596–601.

Klooster J, Yazulla S, Kamermans M. 2009. Ultrastructural analysis of the glutamatergic system in the outer plexiform layer of zebrafish retina. J Chem Neuroanat 37:254–265.

Lin-Jones J, Burnside B. 2007. Retina-specific protein fascin 2 is an actin cross-linker associated with actin bundles in photoreceptor inner segments and calycal processes. Invest Ophthalmol Vis Sci 48:1380–1388.

Lin-Jones J, Sohlberg L, Dose A, Breckler J, Hillman DW, Burnside B. 2009. Identification and localization of myosin superfamily members in fish retina and retinal pigmented epithelium. J Comp Neurol 513:209–223.

Liu X, Ondek B, Williams DS. 1998. Mutant myosin VIIa causes defective melanosome distribution in the RPE of shaker-1 mice. Nat Genet 19:117–118.

Liu X, Udovichenko IP, Brown SD, Steel KP, Williams DS. 1999. Myosin VIIa participates in opsin transport through the photoreceptor cilium. J Neurosci 19:6267–6274.

Liu X, Vansant G, Udovichenko IP, Wolfrum U, Williams DS. 1997. Myosin VIIa, the product of the Usher 1B syndrome gene, is concentrated in the connecting cilia of photoreceptor cells. Cell Motil Cytoskeleton 37:240–252.

Nagle BW, Okamoto C, Taggart B, Burnside B. 1986. The teleost cone cytoskeleton. Localization of actin, microtubules, and intermediate filaments. Invest Ophthalmol Vis Sci 27:689–701.

Nicolson T, Rusch A, Friedrich RW, Granato M, Ruppersberg JP, Nusslein-Volhard C. 1998. Genetic analysis of vertebrate sensory hair cell mechanosensation: the zebrafish circler mutants. Neuron 20:271–283.

Pagh-Roehl K, Wang E, Burnside B. 1992. Shortening of the calycal process actin cytoskeleton is correlated with myoid elongation in teleost rods. Exp Eye Res 55:735–746.

Postlethwait JH, Yan YL, Gates MA, Horne S, Amores A, Brownlie A, Donovan A, Egan ES, Force A, Gong Z, Goutel C, Fritz A, Kelsh R, Knapik E, Liao E, Paw B, Ransom D, Singer A, Thomson M, Abduljabbar TS, Yelick P, Beier D, Joly JS, Larhammar D, Rosa F, Westerfield M, Zon LI, Johnson SL, Talbot WS. 1998. Vertebrate genome evolution and the zebrafish gene map. Nat Genet 18:345–349.

Sahly I, Dufour E, Schietroma C, Michel V, Bahloul A, Perfettini I, Pepermans E, Estivalet A, Carette D, Aghaie A, Ebermann I, Lelli A, Iribarne M, Hardelin J, Weil D, Sahel J, El-Amraoui A, Petit C. 2012. Localization of Usher 1 proteins to the photoreceptor calyceal processes, which are absent from mice. J. Cell Biol. 199:381–399.

Schwander M, Lopes V, Sczaniecka A, Gibbs D, Lillo C, Delano D, Tarantino LM, Wiltshire T, Williams DS, Muller U. 2009. A novel allele of myosin VIIa reveals a critical function for the C-terminal FERM domain for melanosome transport in retinal pigment epithelial cells. J Neurosci 29:15810–15818.

Usher C. 1914. On the inheritance of retinitis pigmentosa, with notes of cases. R. Lond. Ophthalmol. Hosp. Rep. 19:130–236.

Weil D, Levy G, Sahly I, Levi-Acobas F, Blanchard S, el-Amraoui A, Crozet F, Philippe H, Abitbol M, Petit C. 1996. Human myosin VIIA responsible for the Usher 1B syndrome: a predicted membrane-associated motor protein expressed in developing sensory epithelia. Proc Natl Acad Sci U S A 93:3232–3237.

Williams DS. 2002. Transport to the photoreceptor outer segment by myosin VIIa and kinesin II. Vision Res 42:455–462.

Williams DS, Lopes VS. 2011. The many different cellular functions of MYO7A in the retina. Biochem Soc Trans 39:1207–1210.

Wolfrum U, Liu X, Schmitt A, Udovichenko IP, Williams DS. 1998. Myosin VIIa as a common component of cilia and microvilli. Cell Motil Cytoskeleton 40:261–271.

Yacob A, Wise C, Kunz YW. 1977. The accessory outer segment of rods and cones in the retina of the guppy, Poecilia reticulata P. (Teleostei). An electron microscopical study. Cell Tissue Res 177:181–193.

Legends

Figure 1 Ultrastructural analysis of the adult zebrafish outer retina by means of scanning (A-C) and transmission (D-E) electron microscopy. (A) The outer retina of a zebrafish revealing the AOS (arrowheads) as a prominent structure of a cone. The numerous calycal processes (CP, arrows) distributed all around the cone and are markedly thinner than the AOS.(B) Close-up of a COS shows that the AOS starts at the CC and goes alongside the COS. (C) Highly optically magnified AOS showing the folding of the surface area. (D) Longitudinal section of an adult zebrafish cone shows that the AOS is not part of the COS but rather goes alongside the COS. (E) Cross section of the distal part of the cone inner segment shows that the CC is enclosed by a separate membrane bulging around the nine fused triplet microtubules. The CIS is densely packed with mitochondria. Scale bars: A=5µm; B=1µm; C=250nm; D=1µm; E=250nm. AOS, accessory outer segment; CC, connecting cilium; CIS, cone inner segment; COS, cone outer segment.

Figure 2 Development of the accessory outer segment. Cross sections of a 5 day old (A), 12 day old (B) and adult cone (C) show the maturation of the AOS. The surface becomes more enlarged over time and the cytoplasmic bridge between the COS and the AOS is smaller but longer at older stages. In contrast, the CPs are enclosed by a separate membrane at all stages. Scale bars: A,B=500nm; C=1µm. AOS, accessory outer segment; COS, cone outer segment; CP, calycal process; PG, pigment granule.

Figure 3 Radial section of an adult zebrafish immunohistochemically stained with a zebrafish-specific antibody against Myo7a. (A) Myo7a (green) is exclusively found in the outer retina in the area of the cone outer segments. Red channel is autofluorescence. (A') Optical zoom of the outer retina revealing a Myo7a staining in the accessory outer segments of all four cone types. Scale bars: A=25µm, A'=5µm. COS, cone outer segment; dc, double cone; GCL, ganglion cell layer; INL, inner nuclear layer; IPL, inner plexiform layer; lsc, long single cone; ONL, outer nuclear layer; OPL, outer plexiform layer; ROS, rod outer segment; RPE, retinal pigment epithelium; ssc, short single cone.

Figure 4 (A) Structure of zebrafish Myo7a. The different domains and motifs of Myo7a are depicted. Note that zebrafish Myo7a is 2180Aa long with a predicted molecular weight of 252kD. The Myo7a part recombinantly expressed is depicted. The antibody binding site within the second FERM domain is given in red. Abbreviations are: MySc = Myosin motor domain, IQ = Calmodulin binding motif, CC = Coiled-coil domain, MyTH4 = Myosin tail homology 4 domain, FERM = Domain found in **F** for 4.1 protein, **E** for ezrin, **R** for radixin and **M** for moesin, SH3 = Src homology 3 domain. (B) Myo7a1 peptides can specifically block antibody staining against Myo7a1. The top panel shows a regular

Myo7a staining in adult zebrafish AOS (green). Photoreceptors are made visible by overexposure of the red channel, resulting in detectable autofluorescence. In the lower panel Myo7a1 staining in the presence of an excess of Myo7a peptide is shown. Note that AOS staining is completely abolished by incubation with Myo7a peptides. Scale bar equals 10µm. (C) Myo7a1 antibodies recognize recombinant as well as native Myo7a1. In the top panel a western blot on adult zebrafish eye and fin tissue is shown. The antibody reacts with a band of around 260kD in zebrafish eye tissue which correlates well with the predicted size of 252kD. In the lower panel interaction of Myo7a antibodies with the recombinant terminal FERM domain are shown. Note that the antibody recognizes a band of the predicted size in Myo7a1_FERM transfected cells but not in mock transfected controls. (D) AOSs are not enriched in filamentous actin. Adult zebrafish retina sections were stained for filamentous actin (F-actin) using FITC-labelled phalloidin. While faint labelling of F-actin can be seen in cortical structures of blue cones as well as red/green double cones (increased staining at the edges is due the higher number of layers with staining that project into the same area in projections), no labelling resembling the Myo7a labelling of the AOS can be detected. Additional filamentous actin can be detected in the RPE as well as in the area where rods and/or UV cones are located. The red channel represents photoreceptor autofluorescence seen when highly overexposed. Scale bar is 15µm.

Figure 5 Transmission electron micrograph of a radial section of an adult zebrafish stained with a zebrafish-specific antibody against Myo7a. (A) The Myo7a staining is most prominent in the AOS. (B) Optical magnification revealing an intense staining in the AOS and a weak staining in the CC. Scale bars: A=250nm,

B=500nm. AOS, accessory outer segment; CC, connecting cilium; CIS, cone inner segment; COS, cone outer segment.

Figures

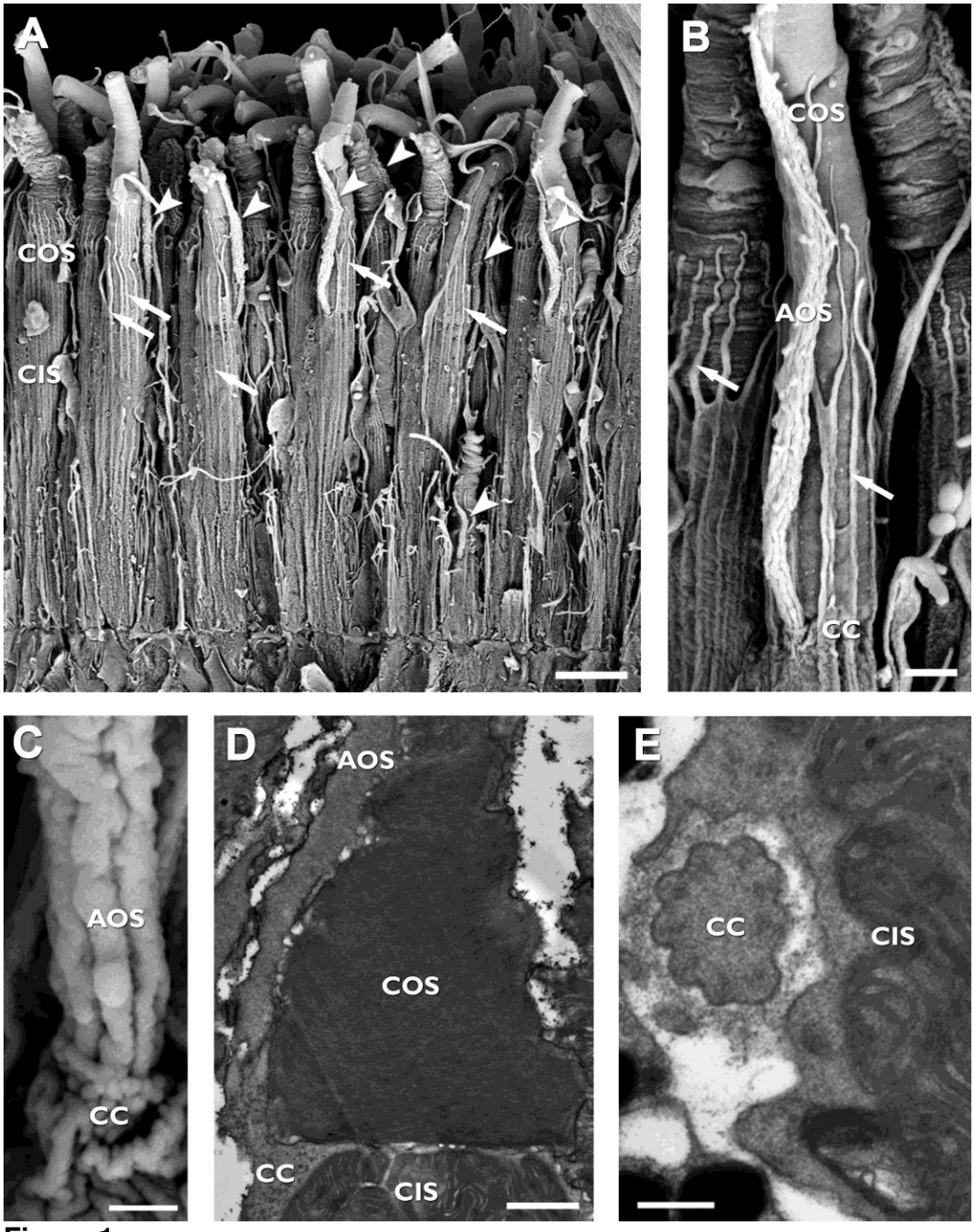

Figure 1

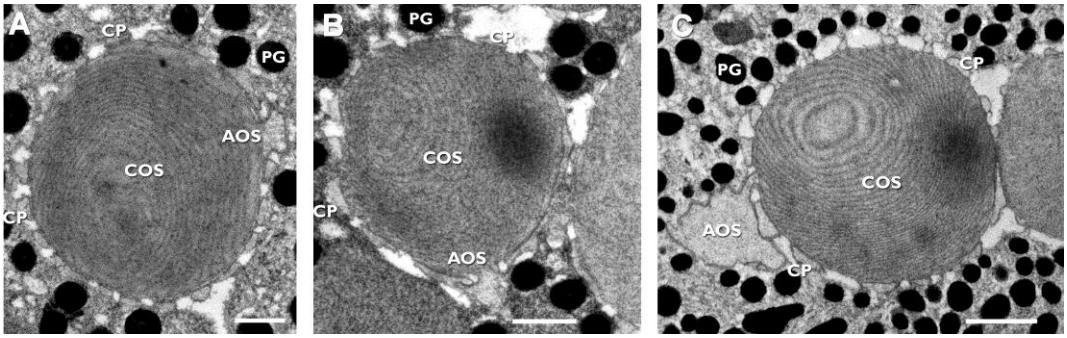

Figure 2

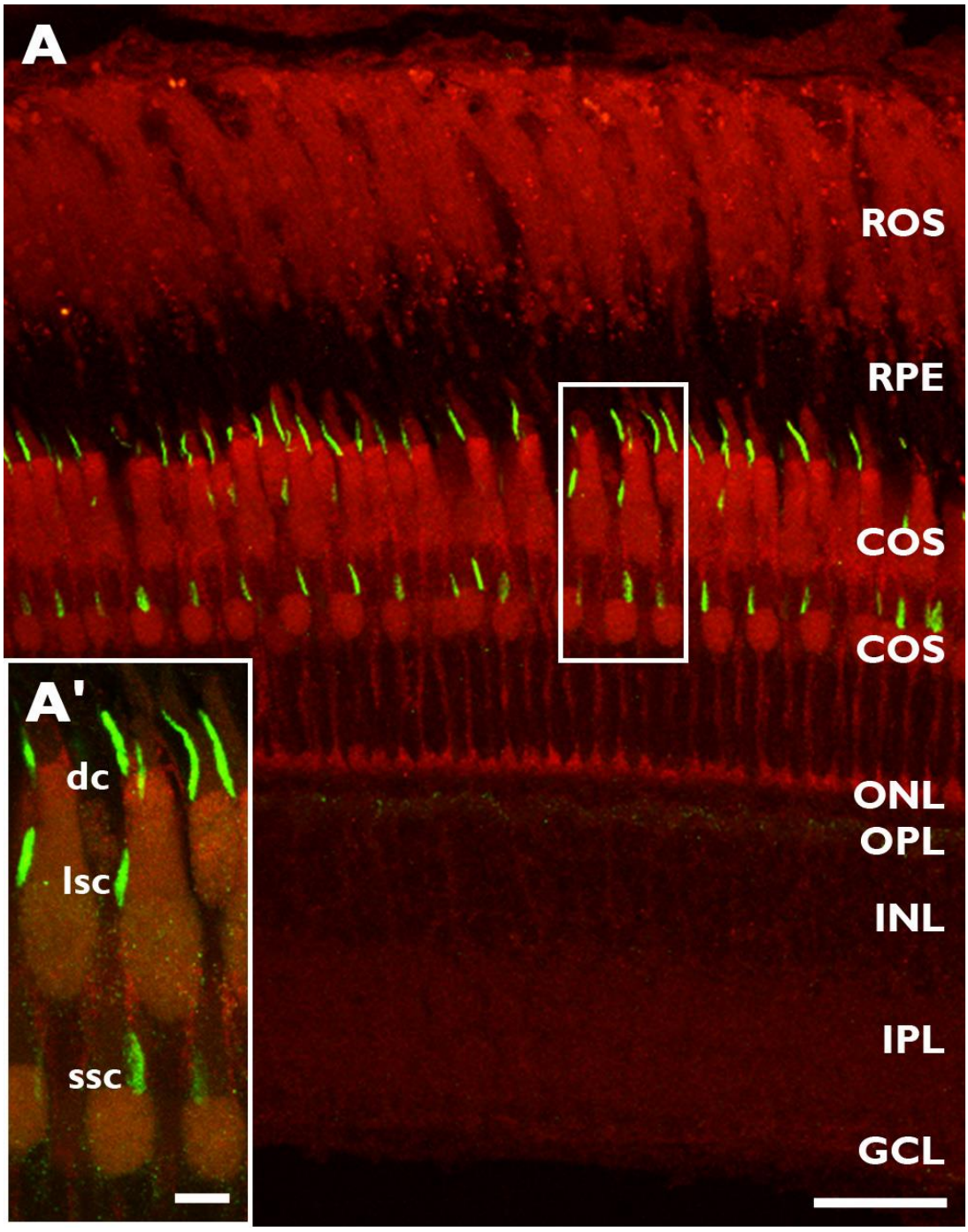

Figure 3

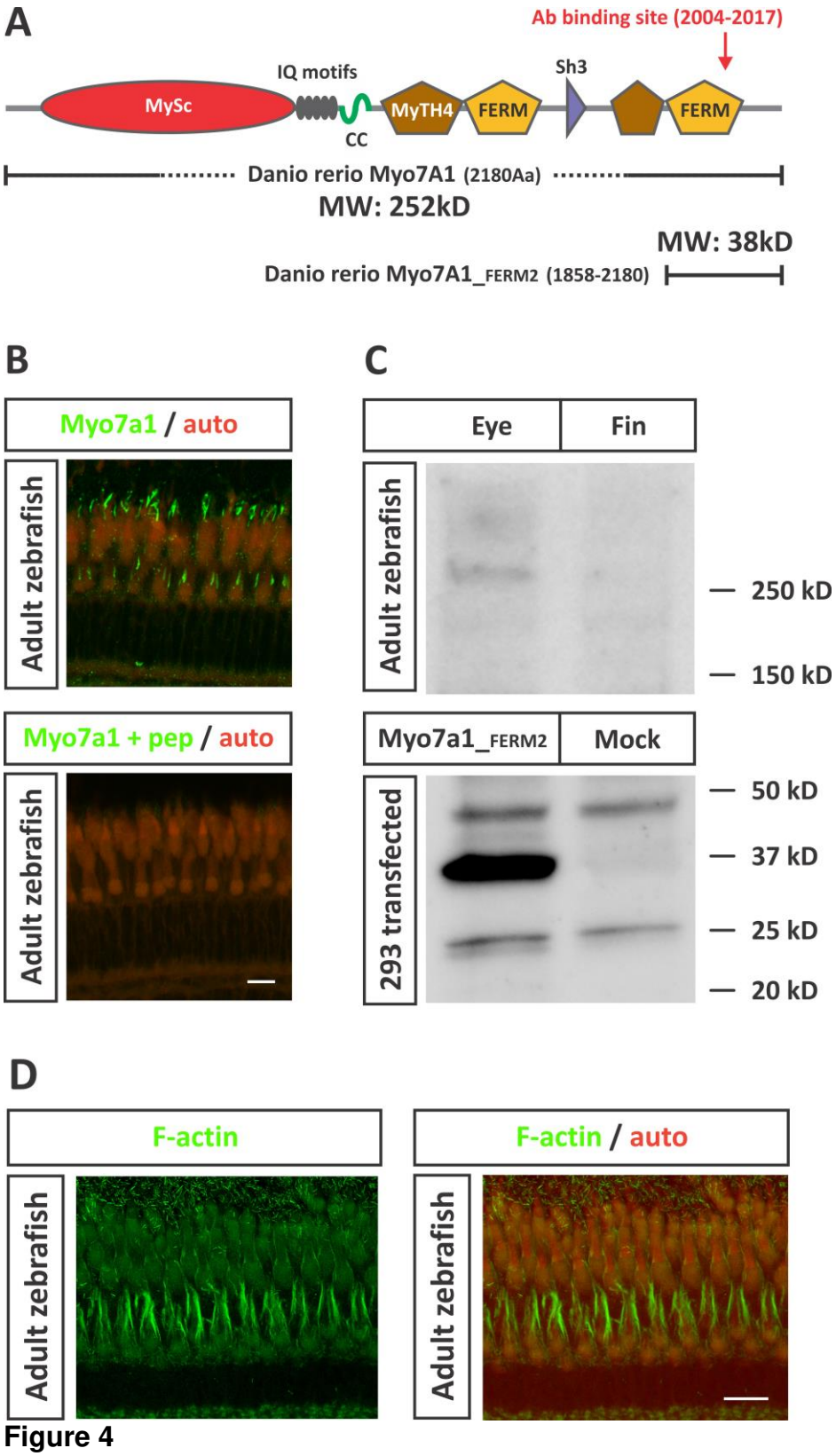
A
Ab binding site (2004-2017)
IQ motifs
Sh3
MyTH4
FERM
FERM
MyTH4
CC
Danio rerio Myo7A1 (2180Aa)
MW: 252kD
MW: 38kD
Danio rerio Myo7A1_FERM2 (1858-2180)
B
Myo7a1 / auto
Adult zebrafish
Myo7a1 + pep / auto
Adult zebrafish
C
Eye
Fin
Adult zebrafish
250 kD
150 kD
Myo7a1_FERM2
Mock
293 transfected
50 kD
37 kD
25 kD
20 kD
D
F-actin
Adult zebrafish
F-actin / auto
Adult zebrafish

Figure 4

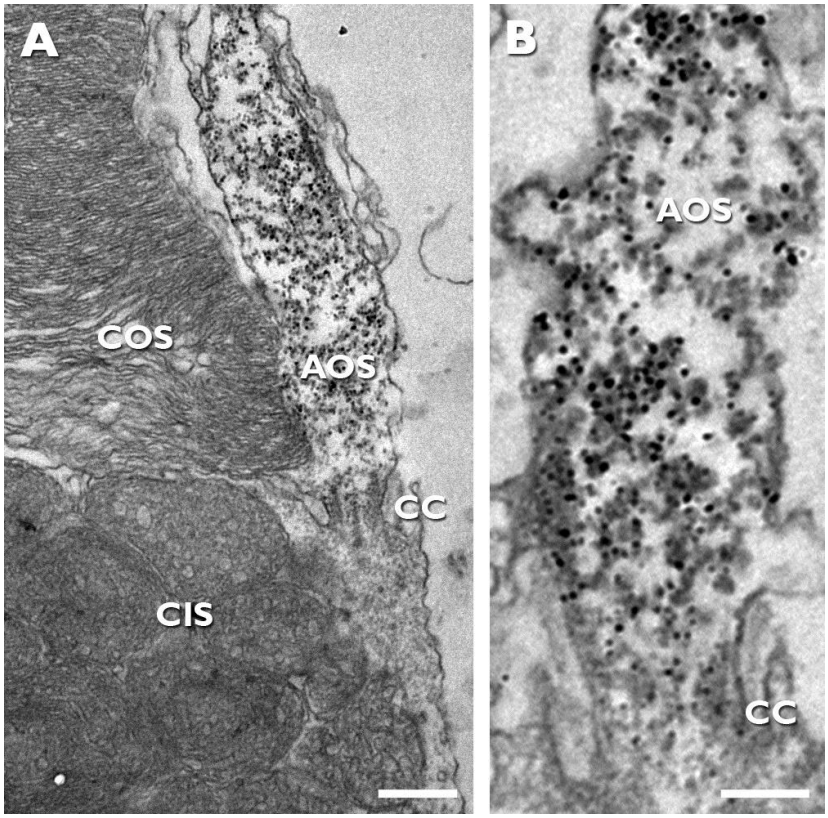

Figure 5